34th Annual International Conference of the IEEE EMBS
San Diego, California USA, 28 August - 1 September, 2012

A Fast Iterative Greedy Algorithm for MEG Source Localization

G. Obregon-Henao [1,*], B. Babadi [1,2], C. Lamus [1,2], E.N. Brown [1,2,3], *Fellow*, *IEEE*, and P.L. Purdon [1,2,*], *Member*, *IEEE*

***Abstract*—Recent dynamic source localization algorithms for the Magnetoencephalographic inverse problem use cortical spatio-temporal dynamics to enhance the quality of the estimation. However, these methods suffer from high computational complexity due to the large number of sources that must be estimated. In this work, we introduce a fast iterative greedy algorithm incorporating the class of subspace pursuit algorithms for sparse source localization. The algorithm employs a reduced order state-space model resulting in significant computational savings. Simulation studies on MEG source localization reveal substantial gains provided by the proposed method over the widely used minimum-norm estimate, in terms of localization accuracy, with a negligible increase in computational complexity.**

I. INTRODUCTION

Magnetoencephalograpy (MEG) and Electroencephalography (EEG) provide measurements of scalp electromagnetic fields generated by cortical currents that reflect neuronal activity at a millisecond time scale [1,2]. However, due to the ill-posed nature of the underlying electromagnetic inverse problem, both MEG and EEG are unable to uniquely localize the generators of this brain activity. Established methods for MEG source localization, such as the minimum-norm estimate (MNE) [3,4], use a Bayesian prior constraint to overcome non-uniqueness and provide instantaneous and independent estimates for each time point. These methods are computationally efficient, but they tend to yield blurred estimates of cortical activity and do not incorporate temporal continuity, which is inherent to the biophysics of the problem. Dynamic source localization methods using an approximation to the Kalman Filter [5], or the Fixed Interval Smoother [6] have been proposed previously. A recent method described by Lamus *et al.* [7] used temporal continuity and neighborhood interaction constraints, alongside an empirical Bayesian algorithm to estimate model parameters in order to improve the spatio-temporal accuracy of the source estimates compared to standard methods.

*Corresponding authors at: 149 13th Street, Room 4.013, Charlestown, MA, 02129, USA, Phone: (617) 643-9515; Fax: (617) 643-9521;
E-mail: obregon@nmr.mgh.harvard.edu
patrickp@nmr.mgh.harvard.edu
[1]Department of Anesthesia, Critical Care, and Pain Medicine, Massachusetts General Hospital, USA
[2]Department of Brain and Cognitive Sciences, Massachusetts Institute of Technology, USA
[3]Harvard-MIT Division of Health, Sciences, and Technology, USA
Research supported by NIH grants DP2-OD006454 (Purdon), K25-NS057580 (Purdon), DP1-OD003646 (Brown), and R01-EB006385 (Brown).

However, this method is computationally costly, due to the Expectation Maximization (EM) algorithm it uses to perform parameter estimation [7]. More generally, these dynamic algorithms do not take into account the sparse nature of brain activity.

In this work, we incorporate techniques from sparsity-based signal processing into the framework of EEG/MEG source localization. In particular, we develop a fast, greedy algorithm for brain source localization based on the class of subspace pursuit (SP) algorithms [8,9]. SP algorithms search for sparse solutions to an under-determined system of linear equations in a greedy [10] fashion by iteratively refining the subspace containing a potential solution. The refinement is carried out iteratively based on a proxy signal obtained from the observation vector. A traditional densely sampled source space (~300,000 sources) is recursively subdivided into Voronoi regions of decreasing size, and given a target sparsity level, the overall algorithm searches for sparse solutions across the hierarchy of source spaces in a nested fashion; Voronoi regions are denoted by spatially compact cortical patches whose lead field mappings are represented by their first few significant eigen-modes [11].

We perform numerical studies of MEG source localization using simulated data (generated using realistic MRI-based head models) within various spatially distributed active regions. These studies reveal significant improvements in both the computational requirements and localization accuracy. For instance, for a given patch with diameter of ~13 mm located over a relevant brain region, with uniform source amplitudes of 10 nAm, and signal-to-noise ratio (SNR) of ~6 dB, our method recovers 100% of the signal power within a small neighborhood of the active region, whereas the MNE only recovers 5% of the power under the same setting.

II. METHODS

A. MEG State-Space Model

We use a distributed source model to represent the set of possible currents underlying the observed MEG measurements. Given a source space S of size M and a total of N sensors, such a model can be expressed as follows:

$$y_t = G(S)x_t + v_t, \qquad (1)$$

where y_t refers to the $N \times 1$ observation vector at time t, G is the $N \times M$ lead field matrix (assuming fixed source orientation normal to the cortical surface) computed from structural MRI data [12], x_t is the $M \times 1$ state vector, and v_t is the $N \times 1$ zero mean Gaussian noise vector with

covariance matrix C. In Eq. (1) we have parametrized the lead field matrix by S, which corresponds to the set of discrete locations in the brain where the currents x_t need to be estimated. It should be noted that the set S, and hence the columns of $G(S)$, are dependent upon the sampling density used to represent the source space. Also, since $M \gg N$, the linear equation lacks a unique solution in general.

We assume that the currents x_t follow a random-walk model:

$$\mathrm{x_t} = \mathrm{Fx_{t-1}} + \mathrm{w_t}\,, \tag{2}$$

where the state transition matrix F represents the state dynamics, and w_t is a $M \times 1$ zero mean Gaussian random vector with covariance matrix $Q = diag(\sigma_1^2, \sigma_2^2, \dots, \sigma_M^2)$. Each σ_i^2, for $i = 1, \dots, M$, corresponds to an unobserved realization from an inverse-gamma distribution, which is chosen as the prior. The initial value x_0 is assumed to be a Gaussian vector with mean μ and covariance matrix Σ. Eq. (1) and (2) define the MEG state-space model.

B. Reduced Order State-Space Model: Cortical Patch Decomposition

Consider the Voronoi regions, or patches $P^1, P^2, \dots, P^K$, induced by the Euclidian norm from a source space of size K over the densely-sampled source space S. Thus, each patch will contain a subset of S, *i.e.*, if S^r is the set of discretized sources within patch P^r, then:

$$\cup_{r=1}^{K} S^r = S\,, \tag{3}$$

and the observation model given in (1) can be rewritten as:

$$y_t = [G^1\, G^2\, \cdots\, G^K] \begin{bmatrix} x_t^1 \\ x_t^2 \\ \vdots \\ x_t^K \end{bmatrix} + w_t, \tag{4}$$

where $G^r := G(S^r)$ and $x_t^r := x_t(S^r)$, for $r = 1, \dots, K$, are the lead fields and sources corresponding to the disjoint patches whose union covers all S, respectively (with possible reordering of the columns of $G(S)$ defined in (1)). Thus, G^r will contain a subset of the columns of G, and x_t^r will refer to the source amplitudes at discrete locations in patch P^r.

Depending on the patch size and the discretized source space density, the columns of G^r, for $r = 1, \dots, K$, will be highly correlated and hence these matrices may be well approximated using a reduced rank representation. The reduced-order singular value decomposition (SVD) [13] of G^r can be expressed as:

$$G^r \approx {U^r}_{N\times p} {D^r}_{p\times p} (V^r)'_{p\,\times\,\dim(x_t^r)}\,, \tag{5}$$

where U^r and V^r are orthonormal matrices, D^r contains the singular values arranged in decreasing order, and the value of p represents the number of significant eigen-modes chosen based on the mean representation accuracy criterion [11] across different patch sizes.

For $r = 1, \dots, K$, let $\theta_t^r := (V^r)' x_t^r$, and,

$$\mathbb{V} := \begin{bmatrix} (V^1)' & 0 & 0 \\ 0 & \ddots & 0 \\ 0 & 0 & (V^K)' \end{bmatrix}_{pK \times \sum_{r=1}^{K} \dim(x_t^r)}. \tag{6}$$

Then, the state and observation equations can be respectively written as:

$$y_t = G_\theta \theta_t + v_t, \tag{7}$$
$$\theta_t = \mathrm{F_\theta \theta_{t-1}} + \widetilde{w}_t, \tag{8}$$

where

$$G_\theta := [U^1 D^1\; U^2 D^2\; \cdots\; U^K D^K], \tag{9}$$
$$\theta_t := [(\theta_t^1)'\,(\theta_t^2)'\,\cdots\,(\theta_t^K)']', \tag{10}$$
$$F_\theta := \mathbb{V} F \mathbb{V}', \text{ and} \tag{11}$$
$$\widetilde{w}_t := \mathbb{V} w_t. \tag{12}$$

Eq. (7) and (8) describe a reduced order MEG state-space model in which the dimension of the state vector θ_t is decreased from M to pK. For example, assume that the 4th recursive subdivision of an icosahedron is used to select a subset of $K \approx 5000$ sources over the original state vector x_t. If these in turn are used as the central vertices for constructing the Voronoi regions, and furthermore each patch is represented by its $p = 2$ most significant eigen-modes, θ_t will lie in a space of dimension ~10000 sources as opposed to the dimension of ~300,000 (corresponding to the dimension of the original state vector x_t). This translates into a substantial decrease in the computational complexity of the inverse problem.

C. Subspace pursuit

We assume that the measured observations result from the superposition of compressible signals coming from a small number of non-overlapping patches. Under this premise, the pursuit algorithm searches for sparse estimates across a hierarchy of source spaces in a nested fashion, using the reduced order state-space model described above, and an extension of the MNE algorithm where the state noise covariance is iteratively updated via EM (sMAP-EM) [7].

A total of $20 \cdot 4^i + 4$ cortical patches with surface areas of approximately $100{,}000/(4^i \cdot 10 + 2)$ mm^2, for $i = 1, \dots, 5$ representing the i^{th} recursive subdivision of an icosahedron, are independently formed over the original densely sampled source space. We denote these nested source spaces by $S_1, S_2, \dots, S_5$, such that $S_1 \subset S_2 \subset \cdots S_5$. Let $G_\theta^{(i)}$ denote the reduced order lead field matrix over tessellation S_i, and $\tilde{G}_\theta^{(i)}$ be equal to $G_\theta^{(i)}$ with normalized columns. The algorithm performs a series of SPs across the observation models induced by each S_i, identifying L sparse components of θ, where L is a level of target sparsity chosen *a priori*. Over the source space S_i with the observation model:

$$y_t = G_\theta^{(i)} \theta_t^{(i)} + v_t, \tag{13}$$

the main steps of the SP algorithm are summarized below:

Table 1. Subspace pursuit algorithm

Input:

$L, G^{(i)}, Y$ ($N \times T$ matrix of observations, where T represents the total number of samples)

Initialization:

1) $P^0 \leftarrow \{L$ indices corresponding to the rows of $G_\theta^{(i)\prime} Y$ with largest l_2-norm$\}$
2) Estimate $\hat{\theta}_{P^0}^{(i)}$ using sMAP-EM restricted to the index set P^0
3) $Y_r^0 \leftarrow Y - G_\theta^{(i)} \hat{\theta}_{P^0}^{(i)}$

Iteration: At the k^{th} iteration, go through the following steps:

4) $\tilde{P}^k \leftarrow P^{k-1} \cup \{L$ indices corresponding to the rows of $\tilde{G}_\theta^{(i)\prime} Y_r^{k-1}$ with largest l_2-norm$\}$
5) Estimate using sMAP-EM restricted to the index set $\tilde{P}^k$
6) $P^k \leftarrow \{L$ indices corresponding to the rows of $\hat{\theta}_{\tilde{P}^k}^{(i)}$ with largest l_2-norm$\}$
7) $Y_r^k \leftarrow Y - G_\theta^{(i)} \hat{\theta}_{P^k}^{(i)}$
8) If $P^k = P^j$, for some $j = \{k-1, \ldots, 0\}$, quit the iteration.

Output:

P^k

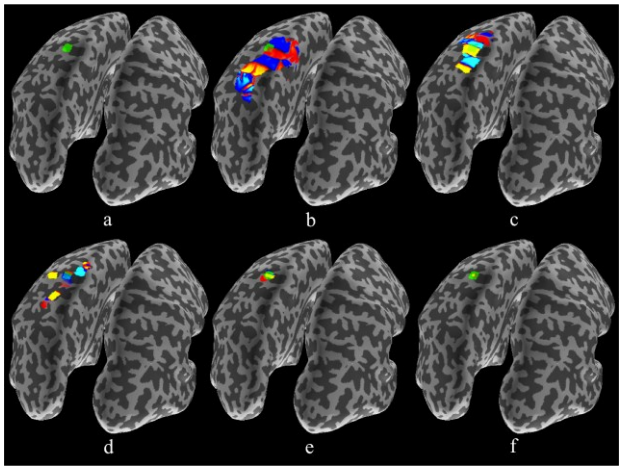

Fig. 1. (a) Geometrical projection of the active region over the inflated cortical surface. (b-f) Progression of the SP algorithm estimates through low rank approximation of a series of nested source spaces. The intensity maps for each subfigure are created using the whole range of the estimated amplitudes (nAm), with bright yellow and bright blue corresponding to the maximum and minimum, respectively.

After computing the output of the SP algorithm over the model of (13), the support of the estimate over S_i together with its nearest neighbors in S_{i+1}, constitute the source space for estimation over the model induced by S_{i+1}. As an example, Figure 1(a) depicts an active region within the somatosensory cortex shown as a geometrical projection over the subject's inflated cortical surface. Figures 1(b-f) show the progression of the SP algorithm, for one instance of time, in search for a subspace to which the inverse solution will eventually be constrained. The full order state estimates are reconstructed as $\mathbb{V}^{(i)\prime} \hat{\theta}_{P^k}^{(i)}$, for all $j \in P^k$, and zero elsewhere. It is important to note that the target sparsity level L depends on the choice of the source space S_i, and is selected based on the expected size of the active region in the corresponding S_i.

When the candidate subspace over S_5 (Figure 1(f)) is obtained, the dynamic Maximum *a Posteriori* EM algorithm (dMAP-EM) proposed in [7] is employed to estimate the activity over the central dipoles in the candidate subspace together with their nearest neighbors.

D. MEG Simulation Studies

We simulated a total of 180 MEG recordings to compare the source localization performance of the MNE and SP solutions for various active regions and different observation noise covariances. Twenty active regions with average radius of ~6.5 mm were randomly created over a highly discretized mesh of ~300,000 dipole sources, *i.e.*, single focal sources defined by their position, orientation, and strength, representing the whole cortical mantle of a human subject. A 10 Hz sinusoidal oscillation (sampled at 200 Hz over a period of 1 s) was used to simulate cortical activity within each region. Dipole moments of 10 nAm were uniformly assigned within each active region in order to be consistent with those that are usually required to explain the magnetic field strengths measured outside the head [14]. For nine different SNR values in the range ± 12 dB, MEG recordings were simulated for each of the 20 active regions according to (1). Finally, the energy ratio within a 5 mm margin of each active region (~1.8 times the radius of the active region) was computed as $\|\hat{\theta}_{IN}\|_F^2 / \|\hat{\theta}\|_F^2$.

The cortical surfaces were reconstructed from high resolution MRIs using *Freesurfer* [15,16]. Sinusoids with uniform amplitudes were used because they constitute a temporal model different than the modeled random walk. A transition matrix F, equal to the identity matrix multiplied by 0.95, was employed. The choice of F was motivated to provide stability to the state model in (2) (see [7] for more details). For each active region and a given SNR value, white Gaussian noise was simulated with an element-wise variance of $\sigma_v^2 := \|GX\|_F^2 / (N \cdot T \cdot SNR)$, where T represents the total number of samples and X is the $M \times T$ state matrix. The *MNE* software package [12] was used to compute the forward solution for each active region, using a single-compartment boundary-element model (BEM) based on high-resolution MRIs, and constraining all dipole orientations to the local normal vector over the cortical surface. The 306-channel sensor layout of the Vectorview MEG system (Elekta-Neuromag, Helsinski, Finland) was employed.

IV. RESULTS

Figure 2(a) portrays a geometrical projection of the active region over the inflated somatosensory cortex. The dMAP-EM estimates (at the same time instant used for Figure (1)) over the subspace obtained from the SP algorithm are shown in Figure 2(b). Finally, Figure 2(c) depicts the estimates obtained from the MNE algorithm over the full order source space S_5.

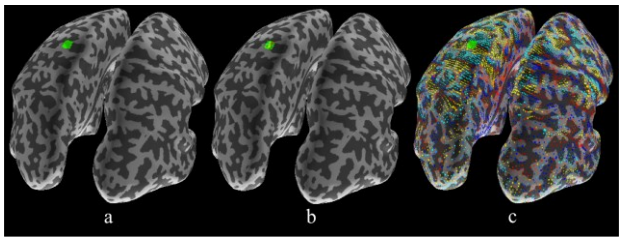

Fig. 2. (a) Geometrical projection of the active region over the inflated cortical surface (b) dMAP-EM estimates over the subspace output by the SP algorithm (c) MNE estimates over the full order source space S_5 of dimension 20484.

The average energy ratio curves for the final SP and MNE estimates across the 20 active regions, as a function of SNR, are shown in Figure 3 (in blue and red, respectively). For an SNR of ~6 dB, which is consistent with MEG measurements [14], an average of more than 77% of the estimated power is attributable to a 5 mm margin of the true cortical regions. The MNE, on the other hand, only assigns about 3% of the estimated energy to the corresponding regions.

For each simulated data realization, the SP algorithm required ~1 minute to localize the support region of the source space, and the dMAP-EM step that followed required ~3 minutes, using a 12-core Xeon workstation. In comparison, the full-dimensional dMAP-EM algorithm requires $\gg$ 50 hours for the same data.

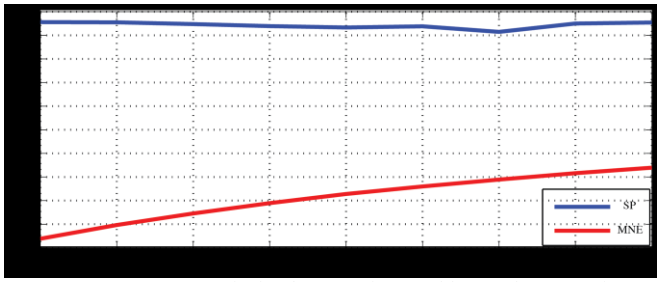

Fig. 3. Average energy ratio for the SP estimates (blue) and MNE estimates (red) across all active regions as a function of SNR. Both axes are in dB units. The SP method provides a 10-20 dB improvement in average energy ratio over MNE.

V. DISCUSSION AND CONCLUSIONS

We derived a greedy algorithm for MEG source localization that is highly effective in localizing the power of cortical activity estimates throughout the human brain by constraining the solution of the neuromagnetic inverse problem to an iteratively identified region. It increases the observability of silent sources by modeling the brain as the union of active regions, as opposed to discretized individual dipoles, and is very robust to noise. Our algorithm possesses the low computational complexity inherent to pursuit algorithms [8], and also generalizes the applicability of pursuit algorithms to the spatio-temporal observation model of MEG. The latter is of utmost importance in real-time applications, such as seizure localization via MEG, as well as the broader applications in brain-computer interface systems.

It is important to note that the 10 nAm dipole moments employed in the simulations are near the practical sensing limit of MEG devices. Nevertheless, our algorithm performs gracefully in this worst-case regime due to its underlying sparsity-enforcing mechanism. Due to their high computational complexity, a comprehensive comparison of our proposed method with other source localization techniques, such as the dMAP-EM algorithm [7], were not feasible. Hence, we chose the widely used MNE algorithm as a comparison benchmark. Further evaluations of the algorithm for multiple active regions, real data, as well as EEG source localization are currently under study.

REFERENCES

[1] M.S. Hämäläinen and R. Hari, "Magnetoencephalographic characterization of dynamic brain activation: Basic principles and methods of data collection and source analysis", In *Brain Mapping: The Methods*, 2nd ed., Academic Press, pp. 227-253, 2002.

[2] D. Cohen and E. Halgren, "Magnetoencephalography," *Encyclopedia of Neuroscience*, vol. 5, pp. 615-622, 2009.

[3] M.S. Hämäläinen and R.J. Ilmoniemi, "Interpreting magnetic fields of the brain: Minimum norm estimates," *Med. Biol. Eng. Comput.*, vol. 32, pp. 35-42, 1994.

[4] A. Dale and M. Sereno, "Improved localization of cortical activity by combining EEG and MEG with MRI cortical surface reconstruction: A linear approach," *J. Cog. Neurosci.*, vol. 5, pp. 162-176, 1993.

[5] A. Galka, O. Yamashita, T. Ozaki, R. Biscay, and P. Valdes-Sosa, "A solution to the dynamical inverse problem of EEG generation using spatiotemporal Kalman filtering," *Neuroimage.* vol. 23, pp. 435-453, 2004.

[6] C.J. Long, P.L. Purdon, S. Temereanca, N.U. Desai, M.S. Hämäläinen, and E.N. Brown, "State-space solutions to the dynamic magnetoencephalography inverse problem using high performance computing," *Ann Appl Stat.*, vol. 5, no. 2B, pp. 1207-1228, 2011.

[7] C. Lamus, M.S. Hämäläinen, S. Temereanca, E.N. Brown, and P.L. Purdon, "A spatiotemporal dynamic distributed solution to the MEG inverse problem," *Neuroimage*, in press, 2012 (Available online 30 November 2011).

[8] W. Dai and O. Milenkovic, "Subspace pursuit for compressive, sensing signal reconstruction," *IEEE Trans. Inf. Theory*, vol. 55, no. 5, pp. 2230-2249, 2009.

[9] D. Needell and J.A. Tropp, "Cosamp: iterative signal recovery from incomplete and inaccurate samples," *Appl. Comp. Harmonic Anal*, pp. 301-321, 2008.

[10] T.H. Cormen, C.E. Leiserson, R.L. Rivest, and C. Stein, *Introduction to Algorithms*, 3rd edition, ch. 16. Cambrige, MA: MIT Press and McGraw-Hill, 2009.

[11] T. Limpiti, B.D. Van Veen, and R.T. Wakai, "Cortical patch basis model for spatially extended neural activity," *IEEE Trans. Biomed. Eng.*, vol. 53, no. 9, pp. 1740-1754, 2006.

[12] M.S. Hämäläinen and J. Sarvas, "Realistic conductivity geometry model of the human head for interpretation of neuromagnetic data," *IEEE Trans. Biomed. Eng.*, vol. 36, pp. 165-171, 1989.

[13] G. Golub and C.F. Van Loan, *Matrix Computations*, 3rd edition. Baltimore, MD: The John Hopkins Univ. Press, 1996.

[14] M.S. Hämäläinen, R. Hari, R.J. Ilmoniemi, J. Knuutila, O.V. Lounasmaa, " Magnetoencephalograpy – theory, instrumentation, and applications to non-invasive studies of the working human brain", *Rev. Mod. Phys.*, vol. 65, pp. 413-497, 1993.

[15] A.M. Dale, B.R. Fischl, and M.I. Sereno, "Cortical surface-based analysis: I. Segmentation and surface reconstruction," *Neuroimage*, vol. 9, pp. 179-194, 1999.

[16] B.R. Fischl, M.I. Sereno, and A.M. Dale, "Cortical surface-based analysis: II. Inflation, flattening, and a surface-based coordinate system," *Neuroimage*, vol. 9, pp. 195-207, 1999.